Catalysis Today 423 (2023) 114002

Contents lists available at ScienceDirect

Catalysis Today

journal homepage: www.elsevier.com/locate/cattod

Optimisation of the processing conditions of hydrolytic hydrogenation of cellulose using carbon nanofiber supported Ni catalysts

E. Frecha, J. Remón, D. Torres, I. Suelves, J.L. Pinilla *

Instituto de Carboquímica-CSIC, C/ Miguel Luesma Castán, 4, 50018 Zaragoza, Spain

ARTICLE INFO

Keywords:
Cellulose
Hydrolytic hydrogenation
Carbon supported catalysts
Nickel
One-pot reaction
Sorbitol

ABSTRACT

The synthesis of sorbitol from cellulose over Ni catalysts is a promising valorisation route in the biorefinery scenario, applying relatively simple preparation methods and earth-abundant metals. The overall selectivity, however, depends on the kinetic control of a complex reaction network, involving the hydrolysis of cellulose to monosaccharides via cello-oligomers, glucose hydrogenation into sorbitol and hydrogenolysis side-reactions of sugars and sorbitol to low molecular weight polyols. Therein, subtle changes in the catalyst composition and process conditions might have a strong impact on the final product distribution. Driven by these challenges, this work first-time provides novel insights into the hydrothermal hydrogenation of cellulose over a carbon nanofibre supported Ni catalyst (Ni/CNF). Firstly, the impact of the duration of a ball-milling pre-treatment step and the influences of the hydrothermal time and temperature were thoroughly analysed. The experimental results obtained highlighted the importance of process control to promote the first transformation of cellulose to glucose and its subsequent hydrogenation to sorbitol to minimise the extension of side reactions. Finally, an additional study was conducted to palliate the recalcitrant nature of cellulose by decreasing mass transfer limitations to a minimum extent. This was achieved by including an additional mix-milling of the amorphous cellulose produced in the first pre-treatment with the catalyst and increasing the H_2 pressure of the hydrothermal hydrogenation process. This allowed attaining a sorbitol yield as high as 62% at 190 °C using an initial H_2 pressure of 8 MPa for 26 h, which is one of the best results reported in the literature.

1. Introduction

The last decades have witnessed a growing interest in utilising lignocellulose biomass as an abundant, inedible and renewable resource for chemicals, materials and energy [1–3]. Out of many processing alternatives, the synthesis of chemicals via platform molecules is one of the most widely envisioned approaches. The strategy suggests a step-wise transformation, whereby biomass is first fractionated into its main components, viz., cellulose, hemicellulose and lignin; and then converted into a limited set of structures that serve as building blocks to furnish a wide range of different chemicals [4–7]. In particular, one of the most valuable intermediates attained from the cellulosic portion is sorbitol, featured in the TOP-12 biomass-derived platform chemicals by the U.S. Department of Energy [8]. It is used as an additive (moisturizer, low-calorie sweetener or emulsifier) in the pharmaceutical, food and cosmetic industries and as the starting material in the manufacture of various fine chemicals, including vitamin C, lactic acid, sorbitan, isosorbide and polyols, and biofuels [9,10].

The synthesis of sorbitol from cellulose can be directly achieved through a *one-pot* process known as hydrolytic hydrogenation. The reaction combines an acid-catalysed initial hydrolysis step yielding glucose, with a subsequent reduction of this species over the metal centres of a catalyst. Given these dual catalytic aspects, various catalysts have been synthesised and tested, including enzymatic, homogeneous and heterogeneous approaches [11,12]. A promising option is based on the integration of hydrothermal hydrolysis with catalytic hydrogenation on supported metal nanoparticles. In this system, the acid-catalysed depolymerisation is achieved by the H protons generated from the aqueous medium at hydrothermal conditions, while the hydrogenation reaction occurs over the metal centres of the catalyst. Such a combination is advantageous, as H^+ can easily diffuse into the intermolecular structure of cellulose with less mass-transfer limitations than solid catalysts [13]. In parallel, the simultaneous hydrogenation of the glucose formed into sorbitol hinders its possible thermal decomposition to by-products.

As expected, the effective integration of homogeneous and

* Corresponding author.
E-mail address: jlpinilla@icb.csic.es (J.L. Pinilla).

https://doi.org/10.1016/j.cattod.2023.01.009
Received 6 September 2022; Received in revised form 7 December 2022; Accepted 11 January 2023
Available online 13 January 2023

heterogeneous catalytic aspects is not an easy task to accomplish, and an overwhelming number of catalytic systems and experimental conditions have been applied, resulting in a wide spectrum of products (hexitols and shorter polyols) [14]. Some of the most representative studies are compiled in Table 1.

Among the platinum group metals (Pt, Rh, Ru, Os, Pd, Ir), Ru and Pt stand as the most effective candidates [17,20,21]. For instance, 2.5 wt% Pt/γ-Al_2O_3 catalysed the conversion of 46% microcrystalline (MCC) cellulose to 25% of sorbitol and 6% of mannitol when the process was conducted at 190 ºC and 5.0 MPa H_2 for 24 h (Entry 1) [15]. Apart from the intrinsic acidity of the support, it was proposed that the hydrogen spillover effect from the metal to the support surface may increase the amount of protonic acid sites and contribute to the hydrolysis step [15,22]. An analogous effect was noted by Luo et al. [16] from the H^+ generated from hot water dissociation at elevated temperatures (245 ºC). Nearly a 40% yield of sorbitol was reached within 30 min at 6.0 MPa of H_2 pressure using supported ruthenium clusters (4% Ru/C) as the hydrogenation catalyst (Entry 2). Similar productivity to hexitols (40%) was reported by Deng et al. after treating commercial cellulose (85% of crystallinity) at 185 ºC and 5.0 MPa H_2 over a 1.0% Ru/CNT for 24 h (Entry 3) [17]. This result was significantly enhanced to 73% (69% sorbitol; 4.0% mannitol) when cellulose was pre-treated with phosphoric acid (85% H_3PO_4, 50 ºC, 40 min) to reduce its crystallinity (33%). Both the metal and catalytic support influence the product yield, since other transition metals (Fe, Co, Ni, Pd, Pt, Rh, Ir, Ag, Au) and metal carriers (SiO_2, CeO_2, MgO, Al_2O_3) resulted in relatively low percentages of sorbitol (in the range of 0–25%, Entries 5–8). Although no information about cellulose conversion was included, the superior H_2 adsorption and spillover ability of a Ru/CNT catalyst were clearly pointed out from H_2-TPD characterisation, with an outstanding (100 μmol/g) amount of H-desorbed species. Such desorption was twice as high as that for the Ru/Al_2O_3 and more than 20-times than those reported for the rest of the catalysts examined [17].

Likewise, many other studies have highlighted the influence of the support on hexitols production [18,20,23]. For instance, a MC-supported Ni catalyst (20% Ni/MC) was significantly more efficient towards the transformation of microcrystalline cellulose than the AC-supported counterpart (20% Ni/AC), Entries 9 vs 10. More precisely, a sorbitol yield of 42.1% was attained after 30 min at 245 ºC and 6.0 MPa H_2, which is comparatively much higher than that obtained with the 20% Ni/AC (19.7%) [18]. In this case, the better behaviour of the 20% Ni/MC was attributed to its mesoporous structure, doubtlessly advantageous for the transportation of large molecules. A compelling approach to reducing mass-transfer effects relies on entangled morphologies, such as carbon nanofibres (CNF) arranged around the cellulose matrix. This peculiar arrangement could improve access to active sites more efficiently than other porous architectures since the entrance of bulky biomolecules inside the catalyst pore system is not required [24]. Based on this concept, the Sel's group managed to convert up to 87% of microcrystalline cellulose at 210 ºC and 6.0 MPa H_2 using a 3.0% Ni/CNF catalyst for 24 h, with a total polyols yield of 55.4% (34.8% of hexitols) (Entry 11) [19]. Also remarkable, such excellent results opened the door for the substitution of noble metals (Ru or Pt) by less-expensive Ni-based catalysts, which are traditionally considered less selective for the synthesis of sugar alcohols, alluding to their hydrogenolysis behaviour [25,26].

In order to elucidate the factors that determined the hexitols selectivity over Ni catalysts, Liang et al. evaluated the catalytic performance of various Ni-supported catalysts. They demonstrated that the hydrogenolysis reaction pathway begins with the dehydrogenation of sorbitol, followed by retro-aldol condensation and re-hydrogenation. Germane to this knowledge, a striking correlation was found between the support acid-basic properties and the initial rate of sorbitol dehydrogenation [27]. In this respect, the use of carbonaceous supports could play a leading role over other alternatives such as metal oxides (Al_2O_3, TiO_2), H-form zeolites (ZSM-5), or functionalised silicas (SiO_2, bentonite) since the lack of acid-base sites suppresses further product degradation by hydrogenolysis [27]. However, these reactions are also sensitive to the reaction temperature and can be equally promoted by the presence of H^+/OH^- dissociated from hot-compressed water, an equilibrium often applied for cellulose decrystallinisation and dissolution [13,20].

To disassemble the polymeric structure and make it more reactive, cellulose can be alternatively subjected to a wide range of pre-treatments, including physical, chemical and biological approaches or a combination of various [28,29]. These methods enhance the accessibility of cellulose through changes in its structural features (particle size, porosity, polymerisation degree and crystalline index) and/or the disruption of the internal cohesion by swelling effects. Such structural alterations resonate on faster cellulose-to-glucose hydrolysis at lower temperatures and/or a larger number of sites for catalytic interactions [30]. Among these pre-treatments, ball- and mix-milling are considered appropriate approaches to palliate the recalcitrant nature of microcrystalline cellulose. Significant improvements in the hydrolytic hydrogenation of cellulose were noted after using pre-treated substrates by ball-milling or mix-milling [20,31,32]. This topic was first researched by Kobayashi et al. on carbon black supported platinum catalysts (5.0 MPa, 463 K, 24 h). By ball-milling the cellulose for 48 h, the conversion raised from 65.6% to 81.9%, while the yield of hexitols increased from 43.1% to 57.7% [20]. The beneficial effect of mix-milling on catalytic results was clearly evidenced by Ribeiro et al., who observed a drastic enhancement in the sorbitol yield from ball-milled cellulose (45%) after 5 h of reaction at 205 ºC and 5.0 MPa H_2 whereas only 14.4% of sorbitol was obtained from untreated samples. This value was further increased to 72% when the Ru/AC catalyst was ball-milled with cellulose [31].

These publications afford valuable information on how different processes and catalytic factors may concur in determining the final sorbitol selectivity over Ni-based catalysts. Besides low dehydrogenation activity, the presence of metallic Ni in the catalyst is the main

Table 1
Cellulose catalytic conversion to polyols in water.

Entry	Substrate (CrI)	Catalyst	Temp. (ºC)	Time (h)	P H_2[a] (MPa)	Conv. (wt%)	Products Yield (wt%)			Reference
							Hexitols	Shorter polyols	Others	
1	MCC	2.5% Pt/γ-Al_2O_3	190	24	5.0	46.0	34.0	9.0	2.0	[15]
2	MCC	4% Ru/AC	245	0.5	6.0	85.5	39.3	41.5	4.8	[16]
3	MCC	1% Ru/CNT	185	24	5.0	*n.r.*	40.0	6.0	*n.r.*	[17]
4	Acid-treated (33%)	1% Ru/CNT	185	24	5.0	*n.r.*	73.0	10.0	*n.r.*	[17]
5	Acid-treated (33%)	1% Ru/Al_2O_3	185	24	5.0	*n.r.*	25.0	14.0	*n.r.*	[17]
6	Acid-treated (33%)	1% Ru/MgO	185	24	5.0	*n.r.*	*b.d.l.*	16.0	*n.r.*	[17]
7	Acid-treated (33%)	1% Ru/CeO_2	185	24	5.0	*n.r.*	7.0	13.0	*n.r.*	[17]
8	Acid-treated (33%)	1% Ru/SiO_2	185	24	5.0	*n.r.*	8.0	*b.d.l.*	*n.r.*	[17]
9	MCC	20% Ni/MC	245	0.5	6.0	84.5	42.1	23.3	19.1	[18]
10	MCC	20% Ni/AC	245	0.5	6.0	61.9	19.7	22.7	19.5	[18]
11	MCC	3% Ni/CNF	210	24	6.0	87.1	34.8	20.6	31.7	[19]

[a] = hydrogen pressure at room temperature; MCC = microcrystalline; *b.d.l.* = below detection limit; *n.r.* = not reported.

requirement to ensure the effective hydrogenation of sugars. Then, understanding the intricacies between cellulose crystallinity, reaction time and temperature becomes mandatory to limit the extent of a large panel of parallel and consecutive side reactions that reduce the hexitol selectivity. The former includes retro-aldol pathways of sugar intermediates and cracking of hexitols to low short-chain polyols via hydrogenolysis. Earlier, we reported mechanistic insights into catalyst design for superior activity in the hydrolytic hydrogenation of cellobiose (i.e., a glucose dimer representative of cellulose) using different Ni-based catalysts supported on carbon nanofibres (Ni/CNF) with a wide range of Ni crystal sizes (5.8–20.4 nm) and loadings (5–14 wt%). A fair compromise between the Ni surface area (3.89 m^2/g) and its resistance against oxidation was found for intermediate crystallite sizes (~11.3 nm) loaded at 10.7 wt%, affording the hydrogenation of 81.2% of cellobiose to sorbitol after 3 h of reaction at 190 ºC and 4.0 MPa H_2 [33]. Taking this information into account, this follow-up study highlights several aspects controlling the hexitols selectivity when cellulose is used as a substrate. These include a first analysis addressing how and to what extent the crystallinity of this solid influence its reactivity under different hydrothermal conditions (temperature and reaction time) and a second study seeking different alternatives to palliate the recalcitrant nature of this substrate. This latter was achieved by decreasing mass transfer limitations to the minimum extension via increasing the H_2 pressure of the system and incorporating a cellulose-catalyst additional mix-milling step. Given the lack of works addressing the hydrothermal hydrogenation of cellulose over Ni-based catalyst, combined with the mechanistic understanding of the effects of pre-and-processing conditions, this work represents a novel contribution in this field.

2. Experimental

2.1. Catalyst preparation

2.1.1. Support synthesis

Fishbone-type carbon nanofibres (CNF) were grown in a rotary bed reactor by catalytic decomposition of synthetic biogas (CDB) on a Ni-Co/Al_2O_3 (33.5:33.5:33 wt%) catalyst, following the methodology elsewhere described [34]. The as-produced CNF were then subjected to a two-step functionalization/purification procedure, first in HCl (60 ºC, 4 h) and then refluxed in HNO_3 (130 ºC, 1 h).

2.1.2. Preparation of the Ni/CNF catalyst

A Ni supported on CNF (Ni/CNF) catalyst, with a nominal Ni loading of 10 wt%, was used in this work. It was prepared by incipient wetness impregnation using nickel nitrate ($Ni(NO_3)_2{\cdot}6\,H_2O$, 98%, Alfa Aesar) as the precursor salt. In practice, an aqueous solution (9.45 mL) of Ni $(NO_3)_2{\cdot}6\,H_2O$ (1.9661 g) was drop-wised to the support (3.5 g CNF). Next, the mixture was ultrasonically dispersed for 10 min and dried at 60 ºC overnight. The fresh catalyst was finally reduced and passivated. To this end, ca. 1.5 g of sample was thermally treated for 1 h at 450 ºC (heating rate of 10 ºC/min) under an inert atmosphere (75 mL STP/min N_2, 99,9992%, Air Liquid), and then reduced at the same temperature by a H_2 stream (100 mL STP/min, 99,9992%, Air Liquid) during 2 h. After cooling to room temperature, the metal surface was passivated overnight by an oxygen-limited stream (O_2/N_2, 1% vol./vol.; 40 mL STP/min, Air Liquid). This stage creates a protective oxide layer around the Ni surface that prevents an eventual bulk re-oxidation upon air exposure. A complete characterisation of this catalyst was recently reported [33].

2.2. Cellulose pre-treatment and characterisation

Prior to the reaction, the accessibility and reactivity of commercial microcrystalline cellulose (Avicel® PH-101, Fluka, 20–100 μm) were enhanced by ball-milling. For this purpose, 6.75 g of cellulose was treated in a planetary mill (Retsch PM 100 CM, Germany), comprising a 50 mL-zirconia jar with 10 balls inside (Ø = 10 mm, ZrO_2). The crystallinity index (CrI) of cellulose was tuned by varying the operation time from 2 to 8 h (including cool down cycles of 10 min after every 50 min of rotation at 600 rpm), and estimated from the XRD pattern by the peak height method developed by Segal *et al.* [35]. The same experimental procedure was followed for the substrate-catalyst (amorphous cellulose-Ni/CNF) mix-milled samples.

The morphology of the cellulose samples with different crystallinities was observed by scanning electron microscopy (SEM, Hitachi S-3400 N). Samples were sputtered with gold before the measurements. XRD patterns were acquired on a Bruker diffractometer (Model D8 Advance, Series 2) in the 2θ range of 5–80° at a scan speed of 4 s/step and a step size of 0.05º using a cooper anode (λ = 1.54056 Å, 40 kV, 20 mA) and a secondary graphite monochromator as the radiation source.

2.3. Catalytic tests, statistical analysis and model fitting

The hydrolytic hydrogenation experiments were conducted in a batch, high-pressure autoclave (Parker Autoclave Engineers, 100 mL), equipped with a PID controller and a magnetic stirrer. In a typical run, an aqueous suspension (30 mL) containing 300 mg of microcrystalline, semicrystalline or amorphous cellulose (depending on the pre-treatment) and 150 mg of catalyst were loaded into the reactor. The autoclave was then sealed, purged and vented with N_2 and H_2, in that sequence. Afterwards, it was pressurised with H_2 and heated to the desired temperature under mild stirring (300 rpm). Zero time was defined when the reaction temperature was reached, the time at which the stirring rate was raised to 1000 rpm. At the end of the test, the reactor was quenched with cold water to stop the reaction as soon as possible (room temperature was achieved in ca. 20 min). The aqueous fraction was separated from the solid products, containing cellulosic matter and the spent catalysts, by vacuum filtration (cellulose, 1.0 μm, Whatman®). The liquid phase was stored for further analysis, while the solid was dried (60 ºC) and weighed.

The catalytic tests include a first analysis (Runs 1–18) of the influences of the reaction temperature (190–230 ºC) and time (3–26 h) on the hydrolytic hydrogenation of cellulose with different crystallynities (CrI, 0–73%), using a cellulose/catalyst ratio of 0.5 g/g and a H_2 pressure of 4 MPa. Subsequently, the influence of the H_2 pressure (4–8 MPa) was assessed for amorphous cellulose incorporating a posterior amorphous cellulose-catalyst mix-milling step of 30 min (Runs 19–22). Such experiments were conducted to decrease diffusional limitations to a minimum extent. The experimental planning for the former study follows a 2-level-3-factor Box Wilson Face Centered (CCF) full factorial design. Accordingly, the number of runs is defined by the expression 2^k, with k being the number of factors, namely, cellulose crystallinity, reaction time and temperature. Six additional axial experiments enabled the assessment of non-linear effects and interactions between the processing variables. Besides, the experimental error and variance were determined through four replicates at the centre point.

Table 2 lists the specific operational conditions for each run and the effective pressure of the system.

The experimental data were analysed using a 95% confidence (p-value = 0.05) Analysis of Variance ANOVA to determine the effects and interactions with statistical significance, using the cause-effect Pareto test to calculate the relative importance of such effects. For both tests, codec variables (between −1 and +1) were utilised, thus making the factors directly comparable. This methodology relates the process variables, namely, cellulose crystallinity (Cr), temperature (T) and reaction time (t), with a given response variable, taking into consideration their individual influence (linear and quadratic effects) and all possible interactions between them. The polynomial expression that describes the models can be generalised as the following equation:

$$y = \beta_0 + \sum_{i=1}^{k}\beta_i x_i + \sum_{i=1}^{k}\beta_{ii}x_i^2 + \sum_{i<j}\beta_{ij}x_i x_j \quad (1)$$

Table 2
Experimental conditions for each run (inlet solution: 300 mg of substrate, 150 mg of catalyst (Ni/CNF) and 30 mL of H_2O).

Run	Cellulose crystallinity (CrI)	H_2 pressure (MPa)	Temperature (ºC)	Effective pressure[a] (MPa)	Time (min)
1	Microcrystalline (78%)	4.0	190	6.5	3
2	Microcrystalline (78%)	4.0	190	6.6	26
3	Amorphous (0%)	4.0	190	6.5	3
4	Amorphous (0%)	4.0	190	6.5	26
5	Amorphous (0%)	4.0	230	7.7	3
6	Microcrystalline (78%)	4.0	230	7.8	3
7	Amorphous (0%)	4.0	230	7.8	26
8	Microcrystalline (78%)	4.0	230	7.8	26
9–12	Semi-crystalline (37.5%)	4.0	210	7.0	14.5
13	Amorphous (0%)	4.0	210	6.9	14.5
14	Microcrystalline (78%)	4.0	210	7.0	14.5
15	Semi-crystalline (37.5%)	4.0	190	6.4	14.5
16	Semi-crystalline (37.5%)	4.0	230	7.7	14.5
17	Semi-crystalline (37.5%)	4.0	210	7.2	3
18	Semi-crystalline (37.5%)	4.0	210	7.0	26
19	Amorphous (0%)	6.0	190	9.2	26
20	Amorphous (0%)	8.0	190	11.4	26
21	Amorphous (0%)[b]	8.0	190	11.4	26
22	Amorphous (0%)[b]	4.0	190	6.4	26

[a] = system pressure at operating temperature.
[b] = mix-milled sample for 30 min at 600 rpm.

where y is the desired response variable, β_0, β_i, β_{ii} and β_{ij} stand for the independent, linear and quadratic terms and linear interactions, whereas x refers to the independent variables (e.g. *CrI, T, t*).

2.4. Product analysis

The analysis of water-soluble products was performed by High Performance Liquid Chromatography (HPLC). The system, LC-2000 Plus Series by Jasco, uses a semi-micro HPLC pump PU-2085, a refractive index detector (Jasco RID-2031) and a column coated with a strong cation-exchange resin (Reprogel Pb, 9 μm, 8 ×300 mm, ReproGel®, Maisch) preceded by a guard-column. Sample separation (volume of 50 μL) was achieved within 56 min using ultrapure H_2O (0.055 μS/cm) as the eluent at a flow rate of 0.5 mL/min, holding the cell temperature and column at 30 ºC and 80 ºC, respectively. Analogous conditions were kept with the analytical standards used for the quantification according to the external standard method. Routinely, the solution was re-filtered before the injection through a 0.45 μm PTFE syringe filter.

A Gas Chromatograph equipped with Mass Spectrometry (GC-MS) and Flame Ionisation (FID) detectors was employed to complement the analysis of reaction products and/or gather additional structural information about unknown products. For this purpose, an Agilent 7890 Instrument equipped with auto-sample and a capillary HP-FFAP column (Agilent) was employed. The GC column was first heated from 60 ºC (holding time of 4 min) to 80 ºC at a ramp rate of 1.5 ºC/min and kept for 4 min. The temperature was then risen to 100 ° C at 3.5 ºC/min, maintained at this point for 10 min and finally ramped to 240 ºC at a rate of 1.8 ºC/min with an isothermal period of 5 min. The chromatographic separation line was followed by an Agilent single quadrupole with an atmospheric pressure chemical ionisation source. Ion mass spectrum was identified using the preinstalled National Institute of Standards and Technology (NIST) reference database. The FID detector was used for quantification purposes, with the products calibrated in the range of 1–5 wt% using pure commercial chemicals. These comprised a series 1,2 alkane diols (propylene glycol (PG), 1,2 butanediol and 1,2-pentanediol).

The gas phase was sampled and analysed by a Micro GC (Varian CP4900), tracing the volumetric composition of CH_4, CO_2, CO and H_2 species. The instrument was fitted with two packed columns (Molecular Sieve and Porapack) and a TCD detector.

2.5. Conversion measurements and product yield

The conversion of cellulose (X) was determined as the weight difference in the solid before and after the reaction (upon subtracting the solid catalyst mass):

$$X_{CELLULOSE}(\%) = \left(1 - \frac{\text{mass of unreacted cellulose}}{\text{mass of cellulose}}\right)\cdot 100 \quad (2)$$

The moisture content of the substrate was taken into account in the mass balance.

The yield of each product (Y) was expressed in wt% and calculated considering the mass of product in the liquid with respect to the initial cellulose fed:

$$Y(\%) = \left(\frac{\text{product mass}}{\text{mass of cellulose}}\right)\cdot 100 \quad (3)$$

3. Results

3.1. Cellulose characterisation

The crystalline ordering of cellulose depends on its origin and pre-treatment [36]. Commercial Avicel® PH-101 cellulose owns a crystallinity index of ca. 78.5% (estimated from the XRD pattern, Fig. 1), which progressively decreased to 37.5% and complete amorphisation after 2 and 8 h of ball-milling at 600 rpm, respectively. This pre-treatment not only disrupts the hydrogen bond network but also modifies the particle size and morphology, leading to a material with higher porosity and external surface area [20,37].

SEM images gave more evidence of some morphological changes

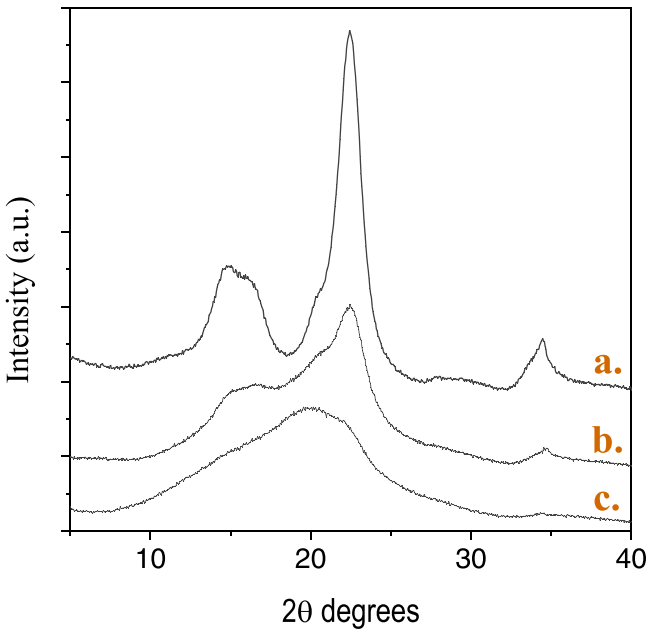

Fig. 1. XRD patterns of commercial cellulose (Avicel PH-101) as a function of milling time: non-treated (a) and ball-milled at 600 rpm during 2 h (b) and 8 h (c).

induced by ball-milling (Fig. 2). Initially, microcrystalline cellulose was present as assemblies of fibrils with a mean size of 50 μm in length (Fig. 2a). A closer inspection of the crystallites reveals that cellulose strands remained stiffly aligned into parallel arrays along the longitudinal axis. The fibres were broken down into smaller fragments as cellulose crystalline features were partly lost (CrI = 37.5% after 2 h of pre-treatment), yet they still showed certain similarities to the original sample (Fig. 2b). After 8 h of ball milling, the total disruption of cellulose backbone was finally noted on its amorphous state (Fig. 2c), forming a crumbled solid with a fairly smooth surface.

3.2. Effect of pre-treatment, time and temperature reaction on cellulose conversion and products distribution

The influences of the reaction time, temperature and cellulose crystallinity were disclosed at a fixed H_2 pressure of 4.0 MPa (room temperature), according to the experimental design defined in Table 2. A detailed account of the cellulose conversion and liquid product distribution for each reaction condition is included in Table 3.

The influence of the cellulose crystallinity for processing times of 3 and 26 h using a reaction temperature of 190 ºC (a) and 230 ºC (b) is shown in Fig. 3. The cellulose conversion and product distribution relied on the reaction temperature, with different outcomes observed depending on the reaction time. At a low temperature (Fig. 3a), the polymeric and crystalline structure of cellulose makes it resistant to hydrolysis. As a result, only 11.7% of conversion was obtained with microcrystalline cellulose after 3 h at 190 ºC (Run 1), which was partially depolymerised into soluble cello-oligomers with shorter chain lengths (3.6%). In parallel, enlarging the reaction time to 26 h (Run 2) increased the conversion of microcrystalline cellulose to 47.5%, yielding cello-oligomers (8.6%) and a small percentage of sugar alcohols (11.4%; including 8.8% of sorbitol and 2.6% of xylitol) as the main products.

Decreasing the crystallinity of the original cellulose to the amorphous state (CrI = 0) via ball-milling (8 h, 600 rpm) boosted the conversion of this material regardless of the processing conditions used in the hydrothermal treatment. Notably, the conversion of ball-milled cellulose (amorphous) is significantly higher than that of the original substrate (37.9% and 88.7% after 3 and 26 h of reaction, respectively). In addition, the formation of sugar alcohols becomes apparent from the earliest stages of the reaction (12.7% after 3 h) to reach a yield of around 49.7% at the end of 26 h (Run 3 vs 4). These species comprise 37.6% of C_6-sugar alcohols and a variety of polyhydric alcohols, such as xylitol (8.6%), erythritol (2.3%), along with low carbon glycols (2.1%, sum of 1,2-propylene glycol and ethylene glycol). The formation of these species comes from two parallel pathways involving the rupture of the glucose backbone followed by hydrogenation and/or hydrogenolysis reactions of sorbitol (vide infra). These data reveal that the influence of the ball-milling pre-treatment depended on the subsequent hydrothermal treatment. While a modest enhancement was attained for a short reaction time (3 h), a substantial improvement in the cellulose reactivity occurred with enlarging the processing time (26 h). Such improvements are accounted for by the positive influence of ball-milling enhancing the accessibility and reactivity of cellulose through the disruption of its crystalline structure, leading to an overall increase in the reaction rate; yet these benefits need long times to be observed.

Using high reaction temperatures is usually effective in accelerating the reaction rate [38,39]. The positive kinetic effect can be explained by a downshift in the ionic product of water at high temperatures, shifting the water equilibrium towards H_3O^+ formation. These species can readily diffuse into the cellulose molecule and facilitate the activation of the glucosidic linkages within the cellulose polymeric structure [13,40,41]. By these means, increasing the temperature upsurged the cellulose conversion regardless of its crystallinity or reaction time (Fig. 3b). Notably, most of the microcrystalline cellulose (85.0%) was converted within 3 h at 230 ºC. Also, the influence of the cellulose crystallinity is less important than that at lower temperatures. While minor differences were observed for a short processing time (3 h), there were no major differences in the cellulose conversion between the crystalline form and the amorphous state when the process was conducted for 26 h. This development is likely due to a weakening of the hydrogen bond network at elevated temperatures (Run 5 vs 6), which disguises the positive influence of the ball-milling pretreatment. However, the positive effect of the temperature on the conversion of cellulose did not go in hand with the selective production of sorbitol, as the exothermic nature of hydrogenation reactions limits sorbitol production at elevated temperatures.

In addition to thermodynamic influences, using lengthy residence times also increases the number of secondary side reactions. For example, the hexitols yield was 16.9–18.7% after 3 h, while only 7.2–8.1 wt% of hexitols was recovered using a reaction time of 26 h in favour of a large spectrum of degradation products, including small quantities of shorter polyols. The sum of C_2-C_5 products ranged between 17.1 and 24.7 wt% in the 3 h-run, remaining almost constant after 26 h. Table 4 lists the specific distribution of such products (Run 5–8). Apart from sugar alcohols, different 1,2 alkane diols (deoxy polyols) were present in the liquid products. These comprised 1,2 hexanediol, 1,2-pentanediol and 1,2-butanediol, whose concentration upsurged from 4.6% at the initial stages (3 h) to 10.9% at the end of the reaction (26 h) when microcrystalline cellulose was used as a feedstock. Overall, the mass balance closed at around 19.4–31.1% upon 26 h, which evidences a rather low carbon utilisation of the starting cellulose.

Scheme 1 gives an overview of plausible routes of sorbitol degradation at high temperatures.

The above experimental analysis has highlighted the convenience of working at mild temperatures (190 ºC) for long residence times (26 h) to selectively transform microcrystalline cellulose into hexitols. However, an initial pretreatment decreased the recalcitrant nature of this material, which allowed using lower temperatures and shorter reaction times. Therefore, the influence of the pre-treatment (ball-milling) duration was disclosed over cellulose samples with different crystallinities at 210 ºC for 14.5 h (Fig. 4, Runs 9–12, 13, 14). As described earlier, the influence of the duration of the ball-milling went in hand with the final

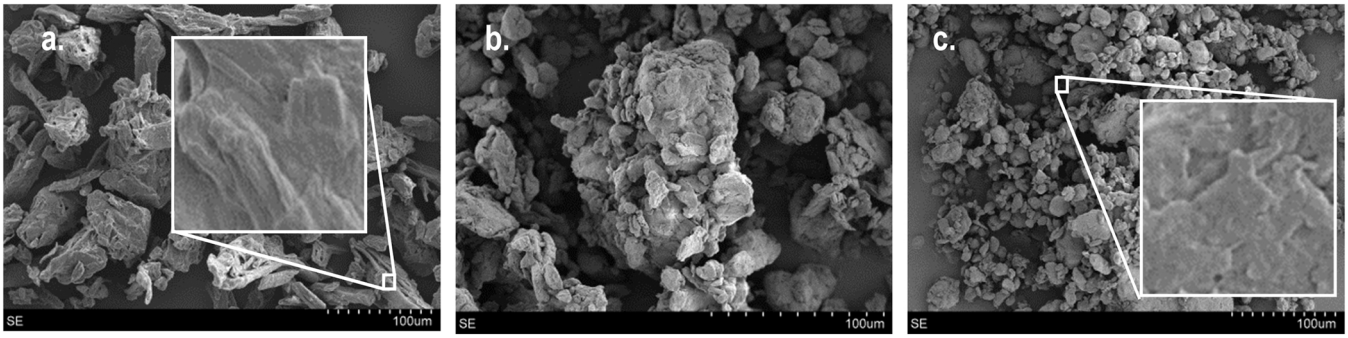

Fig. 2. SEM analysis of cellulose a) non-pretreated, b) intermediate crystallinity (ICr = 37.5%) and c) amorphous. Scale bar = 100 m.

Table 3
Catalytic conversion of cellulose over Ni/CNF under 4.0 MPa H_2 (at room temperature).

	1	2	3	4	5	6	7	8	9	10	11	12	13	14	15	16	17	18
Conditions:																		
Cellulose (CrI)	78	78	0	0	0	78	0	78	37.5	37.5	37.5	37.5	0	78	37.5	37.5	37.5	37.5
Temp. (°C)	190	190	190	190	230	230	230	230	210	210	210	210	210	210	190	230	210	210
Time (h)	3	26	3	26	3	3	26	26	14.5	14.5	14.5	14.5	14.5	14.5	14.5	14.5	3	26
Conversion (wt%)	11.7	47.5	37.9	88.7	97.1	85.0	100	100	94.4	95.6	95.5	96.3	98.9	82.6	63.7	99.7	66.3	99.4
Product yield (wt%)																		
Cello-oligomers	3.6	8.6	19.5	15.1	0.8	10.1	0.7	0.4	2.3	4.8	5.7	0.8	1.8	20.9	10.0	0.3	11.2	6,5
Glucose	0.6	1.1	3.5	b.d.l.	1.1	0.9	1.8	1.0	1.1	1.3	1.6	1.1	1.9	0.8	2.1	2.3	1.3	2.0
Sorbitol	1.5	7.3	9.5	35.5	15.5	15.7	7.8	7.2	10.1	22.5	20.0	10.5	24.8	12.8	22.5	12.9	26.6	18.5
Mannitol	0.9	1.5	0.9	2.1	3.2	1.3	0.2	b.d.l.	0.1	1.9	2.3	3.0	2.5	1.8	1.6	1.8	1.7	b.d.l.
Xylitol	0.7	2.6	2.1	8.6	10.1	6.9	6.1	4.3	7.3	7.8	8.7	7.2	8.9	6.4	5.7	7.3	7.3	7.4
Erythritol	b.d.l.	b.d.l.	b.d.l.	2.3	8.4	5.8	10.7	9.6	6.5	6.9	5.5	7.3	6.5	4.3	0.8	9.5	2.1	7.4
1,2 PG/Glycerol	b.d.l.	0.3	0.2	0.7	2.4	1.7	0.1	5.0	2.6	2.9	2.0	3.6	1.6	1.5	0.4	5.0	0.5	2.3
EG	0.9	b.d.l.	b.d.l.	1.4	3.8	2.8	b.d.l.	7.1	3.8	4.1	3.2	5.7	2.2	2.8	b.d.l.	6.6	b.d.l.	2.8
1,2 alkanediols[a]	0.1	0.3	0.2	2.1	5.5	4.6	1.0	10.9	7.1	7.4	5.0	10.7	3.3	4.5	0.3	10.4	0.7	4.6
CO_2	0.2	0.4	0.2	0.5	1.7	1.2	1.9	1.7	0.4	1.3	1.0	2.0	0.6	0.7	1.3	3.0	0.5	0.6
Others	3.2	25.4	1.8	20.4	44.6	34.0	69.7	52.8	53.1	34.7	40.5	44.4	44.8	26.1	19.0	40.6	14.4	53.8

[a] including 1,2 hexanediol, 1,2 pentanediol and 1,5 pentanediol, 1,4 butanediol and 1,2 butanediol; b.d.l. = below the detection limit; 1,2 PG= 1,2 propylene glycol

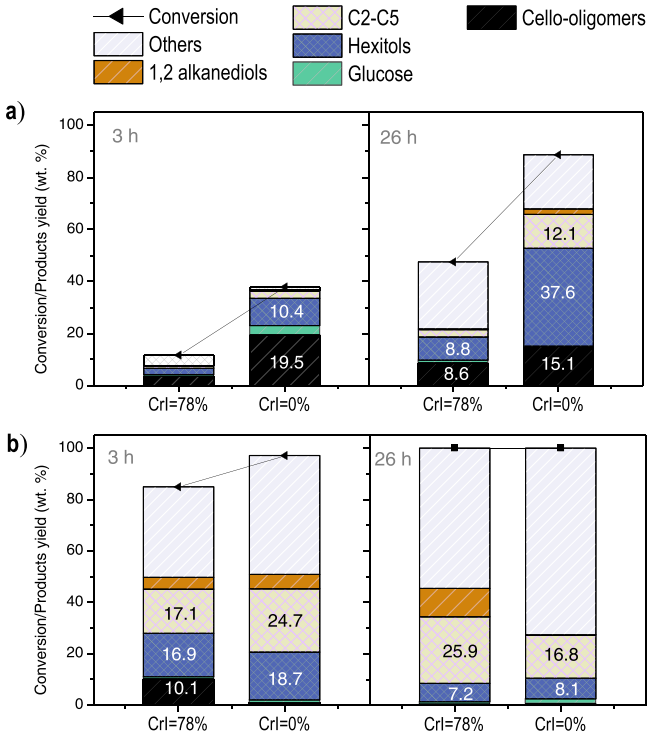

Fig. 3. Catalytic results as a function of reaction temperature, time and cellulose crystallinity a) 190 °C and b) 230 °C.

crystallinity of the pretreated cellulose, and the longer the treatment, the lower was the crystalline index of the material. The experimental results reveal that a progressive decrease in the crystalline index (CrI) from 78% to 37.5% and 0% improved the cellulose conversion and yields to desired products. As for the conversion, the original, untreated cellulose gave the lowest conversion (82.6%), rendering a product spectrum primarily composed of large oligomers (20.9%). A decrease in the crystallinity of the material (i.e., an increase in the ball-milling pretreatment) increased the overall conversion of this solid. Interestingly, no important differences were observed between the amorphous material and the semi-crystalline one (CrI = 37.5%), showing similar conversions (98.9 vs 95.5%) and oligosaccharides yields (1.8 vs 3.4%). However, the yield of hexitols remained higher for the amorphous (CrI = 0%) cellulose (27.3% compared to that 17.5% for the CrI = 37.5% cellulose). These results underline the importance of diffusional aspects governing the hydrothermal hydrogenation of cellulose under heterogeneous catalytic conditions. Thus, a quick transformation of cellulose into glucose units becomes essential to ensure their rapid hydrogenation, avoiding their thermal degradation and/or decomposition to other side products.

The main reactions leading to the formation of side-liquid products are based on the retro-aldol condensation of sugars to aldehydes and ketones through β-C-C bond scissoring [42]. The retro-aldol reaction of glucose generates glycolaldehyde (C_2) and erythrose (C_4), which are then hydrogenated to ethylene glycol and erythritol. If glucose is first isomerised to fructose, then 1,2 propanediol and glycerol are formed with dihydroxyacetone (C_3) as an intermediate (Scheme 2). These compounds may subsequently undergo dehydration or hydrogenation routes to yield a mixture of deoxygenated compounds, as attested by the formation of 1,2 alkane diol in small percentages (7.5% and 3.3% from cellulose with CrI = 37.5% and 0%, respectively).

The influence of the reaction temperature was investigated for cellulose with 37.5% CrI at a residence time of 14.5 h (Fig. 5, Run 9–12, 15, 16). Somewhat predictable, high temperatures facilitated the hydrolysis step, which was reflected by a gradual increase in the cellulose conversion from 63.7% to 95.5% and 99.7% when working at 190, 210 and 230 °C, in that order. The fraction of cello-oligomers simultaneously decreased from 10.0% at 190 °C to 3.4% and 0.3% at 210 and 230 °C, respectively. Nonetheless, an increase in the operating temperature had a detrimental effect on the hexitols selectivity due to two complementary phenomena. On the one hand, such an increase leads to a thermodynamic decrease in the amount of hydrogen solubilised in the aqueous phase hindering hydrogenation. On the other, the number and extension of thermal side reactions increase in relatively harsh conditions. Consequently, the hexitols yield declined from 24.1% to 17.5% and 14.7% at the expense of forming short-chain polyols. The yield of these species was 6.9% at 190 °C, rising to 21.3% at 210 °C and up to 28.4% at 230 °C. A representative distribution of each polyol is shown in Fig. 5 using a temperature of 230 °C. These alcohols comprised similar amounts of xylitol, erythritol, glycerol and ethylene glycol (yields of 7.3%, 9.5%, 5.0% and 6.6%, respectively).

The instability of the hexitols at 210 °C can be confirmed from their temporal evolution profile (Fig. 6, Runs 9–12, 16, 18), which points to catalytic cracking of hexitols into shorter chain alcohols as one of the primary routes for products degradation above 190 °C.

Mechanistically, these reactions take place through various steps, whereby sorbitol is first dehydrated to sorbitan and isosorbide and successively converted into various C_1 and C_5 compounds through hydrogenolysis/dehydroxylation reactions. The C-O cleavage occurs by dehydration routes, whereas the C-C cleavage goes through retro-aldol condensation of unsaturated intermediates [44]. The most common

Table 4
Analysis of variance for response surface model.

Response	R^2	Indep. Term	*A T*	*B T*	*C Cr*	A^2	B^2	C^2	*AB*	*AC*	*BC*	*ABC*	A^2B	AB^2	A^2B^2
Conversion ± 1.26 (%)	0.9993	95.45	17.95	16.55	-9.50	-13.80	-12.60	-4.70	-8.69	6.81	n.s.	3.46	-3.39	6.66	6.56
			(10.64)	(25.91)	(16.09)	(7.92)	(3.57)	(2.42)	(9.94)	(7.06)		(3.42)	(0.37)	(9.13)	(3.54)
Hexitols yield ± 2.76 (wt %)	0.9597	23.21	-1.77	-4.90	-5.20	-5.30	n.s	-3.75	-6.76	4.26	-2.49	2.69	6.56	n.s	n.s
			(12.71)	(2.05)	(13.94)	(7.86)		(6.44)	(1.83)	(11.00)	(23.83)	(10.08)	(10.25)		
C_5-C_2 polyols yield ± 1.59 (wt %)	0.9891	21.25	10.75	5.05	-1.37	-3.60	-6.40	-4.25	-1.39	1.54	n.s	3.29	-3.44	-2.69	6.06
			(11.33)	(26.81)	(11.28)	(1.45)	(6.37)	(4.85)	(8.82)	(1.12)		(5.69)	(0.80)	(21.17)	(0.32)

Numbers in brackets represent the relative influence of each variable (%) according to the Pareto chart.
Response $= \beta_0 + \beta_1 A + \beta_2 B + \beta_3 C + \beta_4 A^2 + \beta_5 B^2 + \beta_6 C^2 + \beta_7 A{\cdot}B + \beta_8 A{\cdot}C + \beta_9 B{\cdot}C + \beta_{10} A{\cdot}B{\cdot}C + \beta_{11} A^2{\cdot}B + \beta_{12} A{\cdot}B^2 + \beta_{13} A^2{\cdot}B^2$
A = temperature; B = time and C = crystallinity; n.s: non-significant with an interval of confidence of 95%.

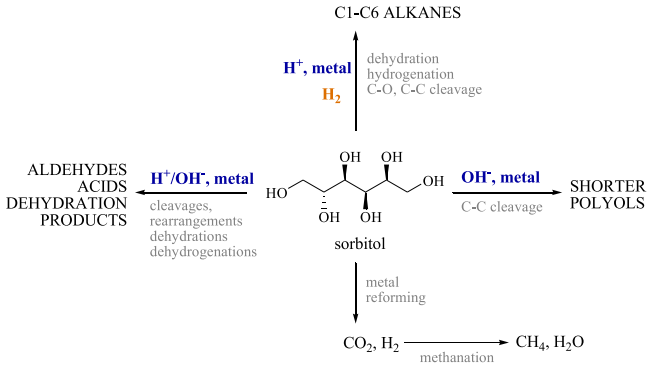

Scheme 1. Sorbitol degradation pathways at high temperatures and in the presence of metal catalysts (
Source: [38]).

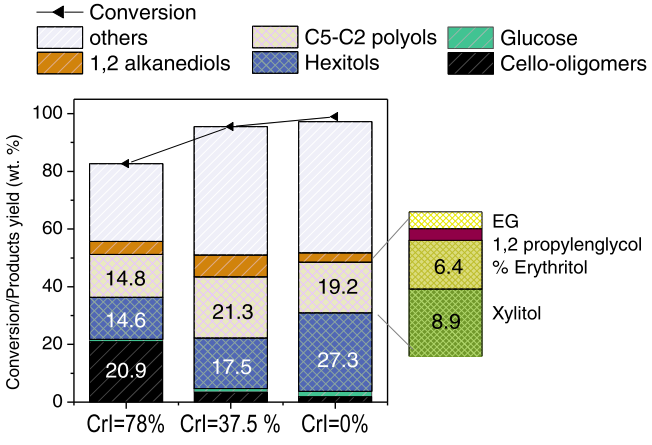

Fig. 4. Influence of cellulose crystalline degree on catalytic conversion at 210 °C and 14.5 h.

products resulting from the hydrogenolysis of sorbitol are illustrated in Scheme 3 [10].

3.3. Statistical analysis and model fitting

From the dataset results, an empirical model was developed to make predictions of catalytic activity within the range of operational conditions used in this work. The three variables chosen as a response were the cellulose conversion, yield of hexitols and short-chain polyols (C_2-C_5). The values of the coefficients determined for the regression models for each response variable, along with the relative importance of all terms statistically significant, are tabulated in Table 4. The goodness of fit of these models was supported by regression coefficients (R^2) close to the unit in all the cases (R^2 = 0.999, 0.960 and 0.989 for cellulose conversion, yield of hexitols and C_2-C_5 polyols) and their insignificant lack of fit (p-values of 0.11, 0.33 and 0.22 for the cellulose conversion and the yields of hexitols and C_2-C_5 polyols, respectively). The surfaces created from these models describing the influence of the processing conditions on the cellulose conversion and the yields of hexitols and short-chain (C_2-C_5) polyols can be visualised in Figs. 7–9.

The impact of the processing variables on the cellulose conversion, based on the Pareto test, ranked to the following extent: residence time (25.9%), crystallinity degree (16.1%) and reaction temperature (10.6%). Additionally, the linear and quadratic interactions of the reaction time with the temperature were equally important (9.9% and 9.1% for *T-t* and *T-*t^2, respectively). These influences are graphically presented in Fig. 7. As a general rule, cellulose conversion gradually increased with enlarging the reaction time and/or augmenting the temperature irrespective of the cellulose crystallinity. However, the magnitude of such variations depended on the cellulose crystallinity. The former means that more severe conditions were required for the entire transformation of untreated (crystalline) samples. For instance, the integral conversion of amorphous cellulose was reached in 15.8 h at 207 °C, whereas 24.4 h and 227 °C were required to degrade crystalline cellulose completely (conversion >99%).

The yields of hexitols primarily relied on the cellulose crystallinity and reaction temperature (13.9% and 12.7%, respectively), with the reaction time having a comparatively lower impact (2.1%). Nevertheless, the most significant influence (23.8%) was exerted by the linear interaction between the cellulose crystallinity and reaction time (*t-Cr*). Additionally, some temperature interactions with other parameters (*T-Cr*, T^2*-t*, *T-t-Cr*) also had a significant influence, although their impact was less influential (ca. 10%). Fig. 8 shows the influence of these variables and interactions on the yield of hexitols using 3D surfaces and contour plots. Such representations also show how the yields of hexitol substantially depended on the cellulose crystallinity index. An increase in the crystallinity substantially decreased the hexitols production regardless of the temperature or reaction time. In addition, irrespective of the starting material, the response surface plot depicted the same turning point at ca. 210 °C for short-time runs (3 h). Accordingly, the proportion of hexitols at short contact times increased with increasing the process temperature from 190 to 210 °C, whereas using higher temperatures caused a decrease in the hexitols production in favour of forming shorter polyols (C_2-C_5). The effect of reaction time was strongly

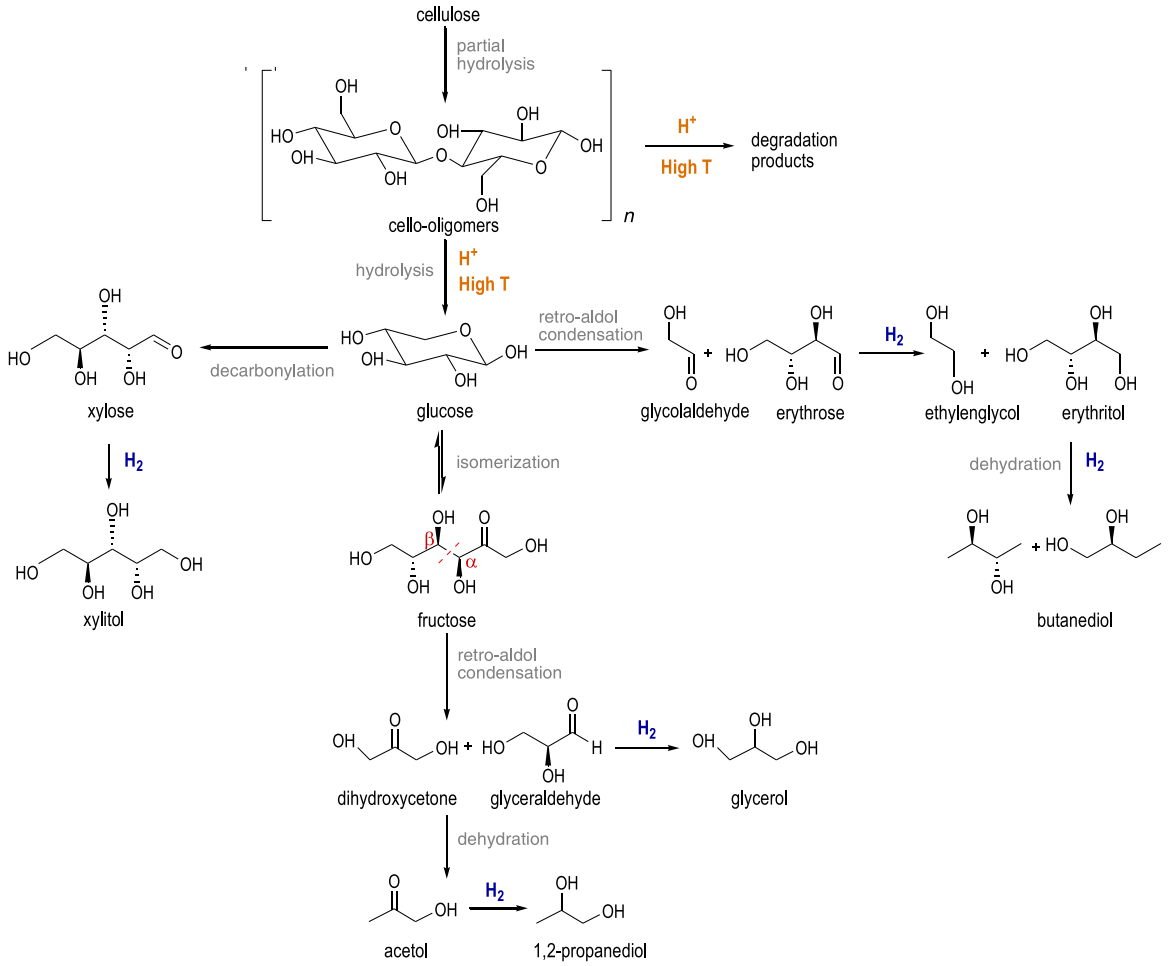

Scheme 2. Reaction routes for glucose degradation in the presence of hydrogen and metal catalysts
Adapted from [43].

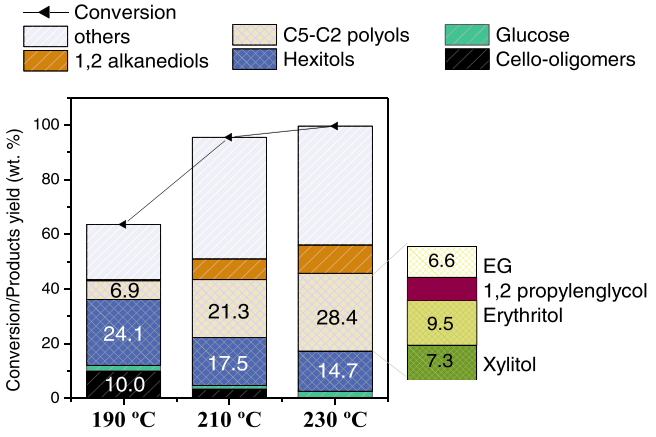

Fig. 5. Influence of reaction temperature on the catalytic conversion of cellulose (CrI= 37.5%) after 14.5 h.

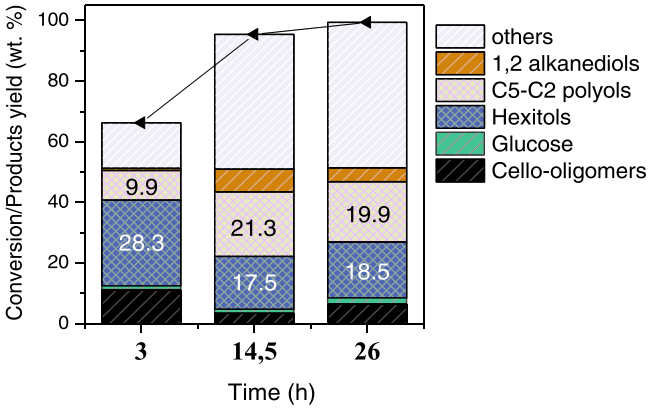

Fig. 6. Conversion profile of cellulose (CrI = 37.5%) at 210 °C.

dependent on the reaction temperature. At mild conditions (190 °C), the hexitols yield linearly increased with enlarging the processing time. The magnitude of these variations was substantially more marked for amorphous than untreated cellulose (remaining practically unchanged). An opposite tendency was observed at temperatures above 200 °C, indicating that degradation of hexitols occurred substantially.

In quantitative terms, the hexitols yield ranged from 3.5 to 39.0 wt% with a deviation standard of 2.8. The best value was attained from amorphous cellulose at the lowest temperature (190 °C) and the longest residence time (26 h) of the experimental plan. Based on statistical calculations, such operational conditions should coincide with an optimal scenario to produce the maximum theoretical yield of hexitols (39.0% at 87.9% of cellulose conversion), working under unlimited conditions of ball-milling duration or reaction time. However, a closer look at the contour plots reveals that some other runs can be conducted at a considerably shorter timeframe, either by reducing the duration of the reaction or the previous pre-treatment, without strongly affecting

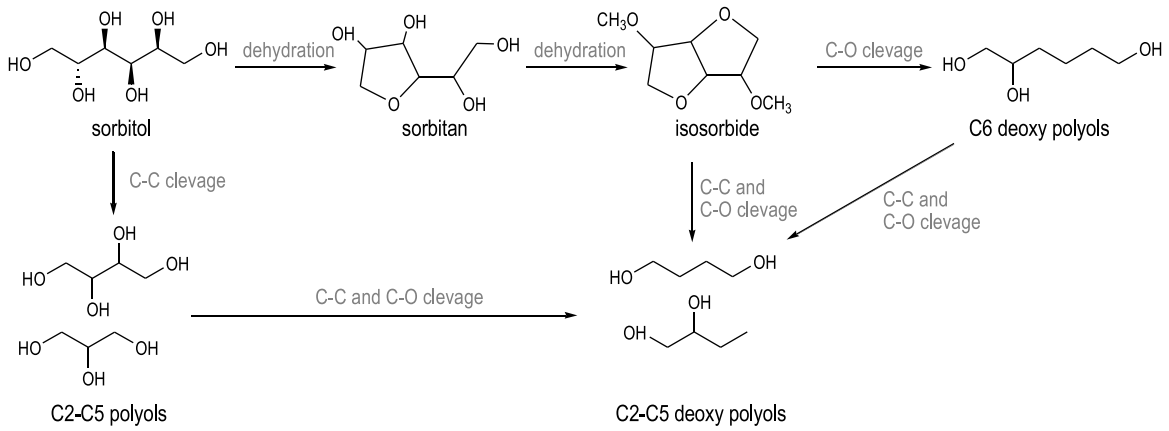

Scheme 3. Major reaction pathways of sorbitol hydrogenolysis (Source: [6]).

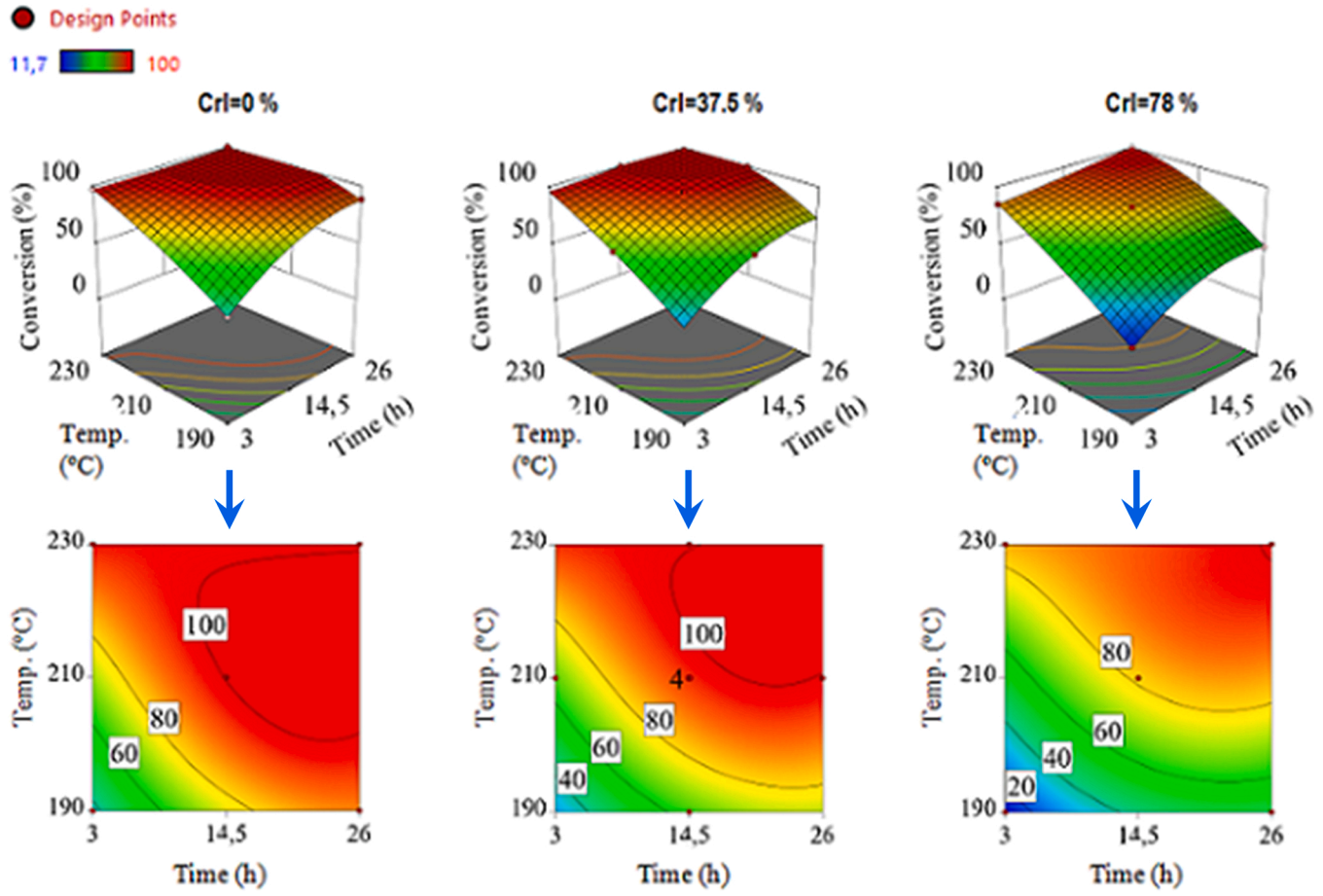

Fig. 7. Response surface for cellulose conversion with different crystallinities.

the yield. One of the most conservative possibilities relies on the amorphous cellulose treatment at 190 °C for a shorter time (19.6 h) at the expense of a small decrease in the hexitols fraction (31.4%). A more pragmatic solution but comparatively less ambitious is the synthesis of 26% of hexitols from amorphous cellulose after only 3 h at 205.6 °C. In addition, it is possible to transform up to 22.5% of raw cellulose to hexitols at a reaction temperature of 216.4 °C for 3 h, avoiding the need for an additional ball-milling stage for cellulose amorphisation.

Following the preceding discussion, short-chain (C_2-C_5) polyhydric alcohols arise from two main degradation pathways, namely, retro-aldol reactions of intermediate saccharides and hydrogenolysis of hexitols at temperatures from 210 °C onwards. Both contributions converged at a maximum value of 28% obtained from semi-crystalline cellulose after 14.6 h at 230 °C (Fig. 9). At this point, the total yield of sugar alcohols (including hexitols) reached 43% at a conversion level of 99.6%. According to the Pareto calculations, the most influential independent variable was the residence time, with a relative contribution (26.8%) twice more significant than those of the cellulose crystallinity (11.3%) or reaction temperature (11.3%). As regards the detailed influences of the processing conditions on the yields of short-chain (C_2-C_5) polyhydric

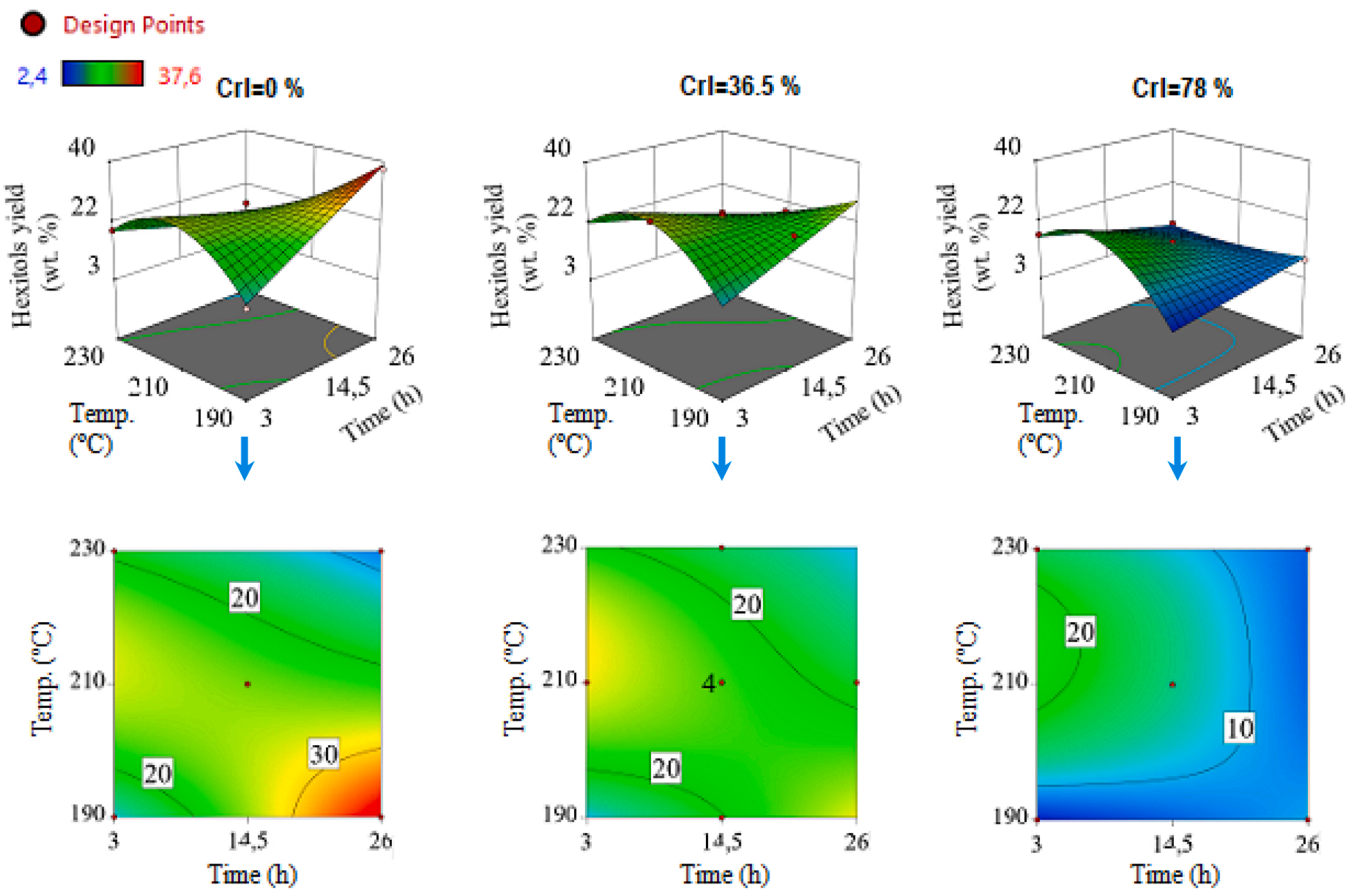

Fig. 8. Response surface and contour plot of hexitols yield obtained from cellulose with different crystallinities.

alcohols, Fig. 9 shows that increasing the reaction temperature upsurged the yield of these species regardless of the reaction time or cellulose crystallinity. The influence of the reaction time was particularly important when amorphous (CrI = 0%) cellulose was used as a feedstock. In this case, while increasing the reaction time promoted the formation of C_2-C_5 polyhydric alcohols at a low temperature (190 °C), the same enlargement led to a decrease in the yields of these products when a high temperature (230 °C) was used. Such differences are accounted for by the different influences of the reaction time on the process, promoting the formation or decomposition of these species depending on the reaction temperature. Additionally, the impact of the cellulose crystallinity on the yields of these short-chain alcohols was less critical, which can be observed by comparing the 3D plots for the different samples. However, the cellulose crystallinity altered the influence of the reaction time on the process. For semi-crystalline (CrI = 37.5%) cellulose, the influence of the reaction time was not essential from a practical point of view. On the contrary, when microcrystalline (CrI = 78%) cellulose was used as a feedstock, the influence of the reaction time was particularly important at high (210–230 °C) temperatures. Under such conditions, lengthening the reaction time augmented the yields of short-chain polyhydric alcohols.

To sum it up, three main scenarios can be depicted from the theoretical optimization, making use of the empirical models developed with the ANOVA analysis. The first optimisation aims to maximise the hexitols productivity under unlimited conditions of processing time (reaction time and pre-treatment duration), whereas Optimisation 2 is directed towards the production of shorter polyols. A combined optimum that maximizes the production of total polyols (C_6-C_2) was finally sought in Optimization 3. In order to meet these criteria, a relative importance from 1 to 5 has been assigned to each constraint. Table 5 compiles the three main scenarios built from the theoretical optimization, targets and the reaction conditions that satisfy the conditions.

Optimisation 1 shows that the maximum productivity to hexitols (39.0%) is achieved after 26 h of reaction at 190 °C starting from cellulose in an amorphous state, i.e., pre-treated by ball-milling for 8 h. Besides, 14.2% of shorter polyols are formed.

In some cases, the synthesis of smaller molecular polyols (C_5-C_2) may be of interest. The theoretical predictions revealed that converting semi-crystalline cellulose (CrI=38.5%) at 230 °C for 14.6 h leads to the highest value of C_2-C_5 polyols (28.4%), along with small amounts of hexitols (16.1%), Scenario 2. Additionally, Optimisation 3 suggests that the formation of hexitols (22.6%) and C2-C5 polyols (24.9%) can be maximized concurrently at 220.1 °C for 12.4 h using cellulose with a crystallinity index of 27.9%.

3.4. Decreasing mass transfer limitations: Increasing the H_2 pressure and incorporating a cellulose-catalyst mix-milling step

The preceding results have shown how the successful conversion of cellulose into sorbitol was primarily conditioned by the efficient conversion of cellulose to glucose and its ready hydrogenation into sorbitol to avoid forming side products. This relies on the high instability of the unsaturated acid aldehyde, which must be immediately hydrogenated or else degradation reactions are deemed to occur. However, the rapid hydrogenation of sugars might be particularly challenging when bulk molecules such as cellulose are processed. In fact, even starting from a highly accessible (amorphous) substrate and using a catalyst with proven hydrogenation ability, the maximum yield of hexitols from cellulose was not substantially high (38%). Besides, the formation of by-products was significant (yields of 21%). Given these challenges, a final set of experiments was performed to palliate these inherent mass-

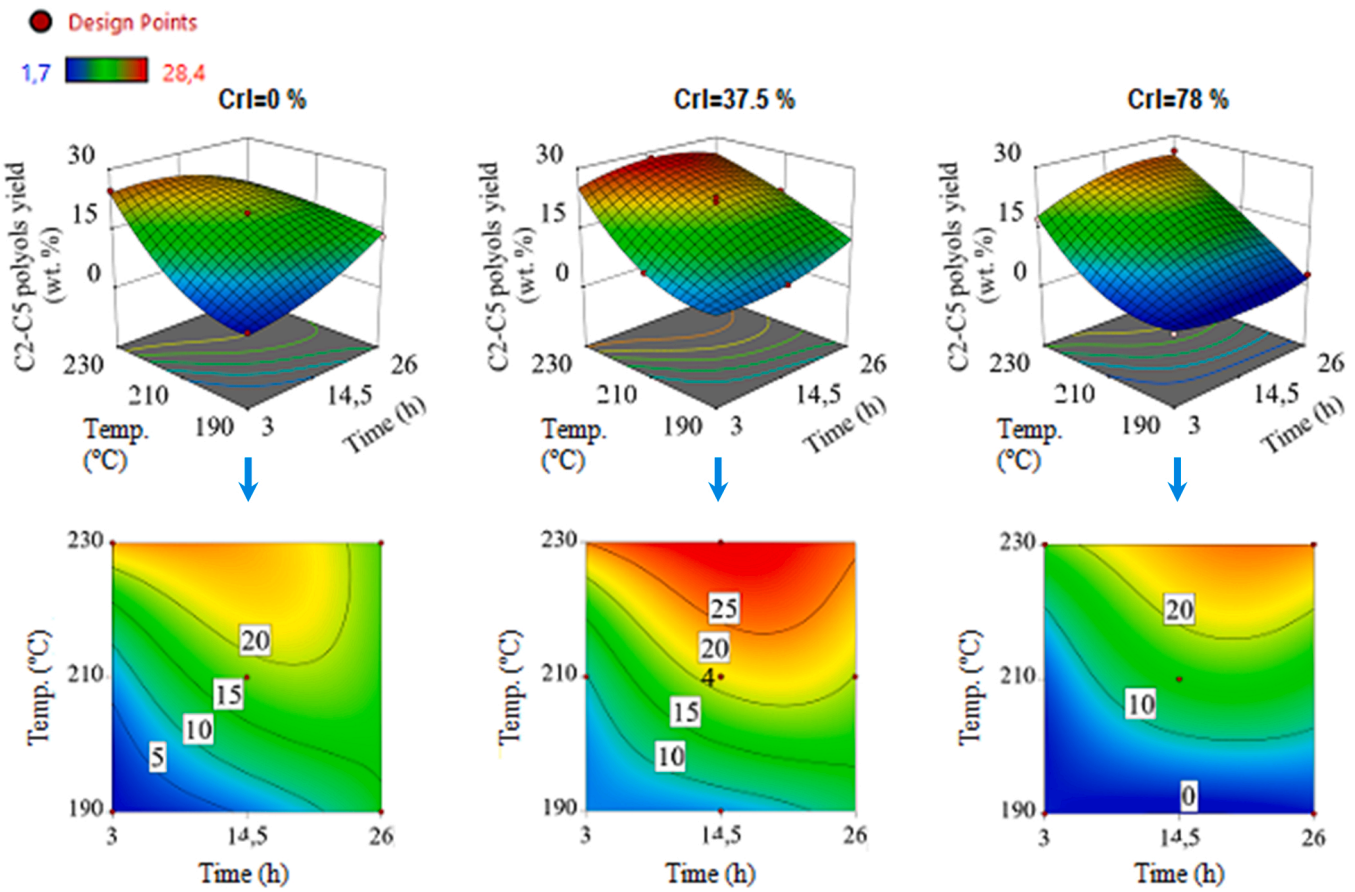

Fig. 9. Response surface for the production of C_2-C_5 polyols obtained from cellulose samples with different crystallinities.

Table 5
Theoretical optimisation: objectives, relative importance (from 1 to 5) and the optimal solution predicted by the model (operational conditions and response variables).

	Cellulose crystallinity[a] (%)	Temp. (°C)	Time (h)	Cellulose conversion	$Y_{HEXITOLS}$ (wt%)	$Y_{C2\text{-}C5\ POLYOLS}$ (wt%)
Scenario 1						
Target	None	None	None	Max.	Max.	Min.
Importance				2	5	2
Solution	0	190	26	87.9	39.0	14.2
Scenario 2						
Target	None	None	None	Max.	None	Max.
Importance				2		5
Solution	38.5	230	14.6	99.6	16.1	28.4
Scenario 3						
Target	None	None	None	Max.	Máx.	Max.
Importance				2	5	5
Solution	27.9	220.1	12.4	100	22.6	24.9

[a] Inversely correlated with the ball-milling duration

transfer limitations.

From a theoretical viewpoint, the catalytic hydrogenation of sugars involves a three-phase catalytic system, in which H_2 gas is first solubilised in the aqueous phase and then diffuses to the liquid-solid interface of the metal catalyst. Activated H species finally interact with the hemiacetal group of saccharides on the external surface of the support [11,45]. In this layout, liquid-solid mass transfer limitations can be partially ameliorated with a large excess of molecular species ($H^{\bullet}$) in the vicinity of the catalyst and the substrate, which can be achieved using high gas external pressures. In order to ascertain whether or not this hypothesis is valid for this system, the initial H_2 pressure was gradually increased in the range of 4.0–8.0 MPa, processing amorphous cellulose for 26 h at 190 °C. Fig. 10a shows how increasing the initial H_2 pressure markedly improved the yield of hexitols from 37.6% (4.0 MPa) to 40.4 (6.0 MPa) and 54.3% (8.0 MPa). This confirms that the hydrolytic hydrogenation of large macromolecules such as cellulose faces severe H_2-diffusion internal resistances. Table 6 details the specific product distribution, with xylitol as the second major product (yield of 8.2–8.6%), followed by erythritol (yield of 2.1–2.7%).

A subsequent strategy was followed to mitigate internal mass-transfer limitations further. This comprised an additional mix-milling step of the catalyst and substrate (amorphous cellulose) for 30 min. Overall, the practice of mix-milling can reduce mass transfer limitations in two complementary ways. First, it promotes the production of water-soluble oligosaccharides, which are more amenable to hydrolysis. Secondly, the more intimate contact between the solid feedstock (cellulose

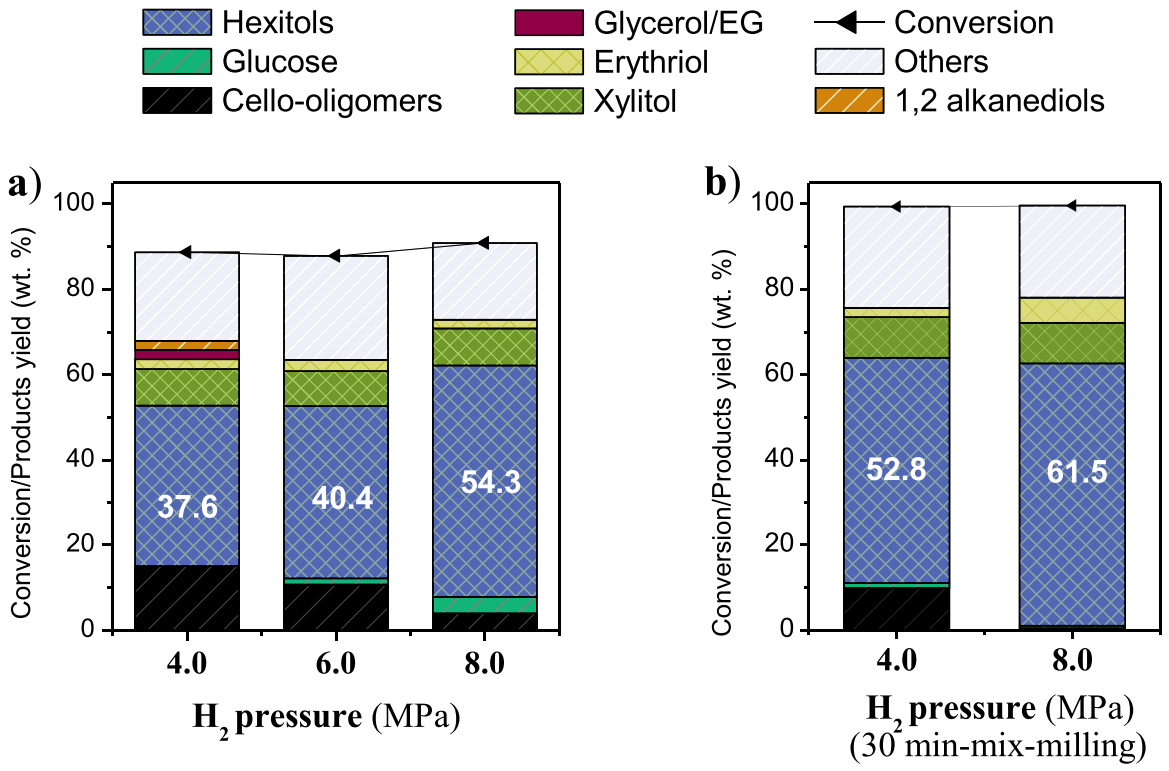

Fig. 10. Effect of H_2 pressure on catalytic results. Reaction conditions: 190 ºC, 26 h, amorphous cellulose.

Table 6
Influence of H_2 pressure on cellulose conversion and product distribution after 26 h at 190 ºC.

H_2 pressure (MPa)	X (%)	$Y_{PRODUCTS}$ (mass %)							
		Cello-oligomers	Glucose	Sugar alcohols[a]					Others
				C_6	C_5	C_4	C_3	C_2	
4.0	88.7	15.1	< l.d.	37.6	8.6	2.3	2.2	1.4	20.8
6.0	87.9	10.7	1.5	40.4	8.2	2.7	n.d	n.d	24.4
8.0	90.9	3.9	3.9	54.3	8.6	2.1	n.d	n.d	18.05
4.0[b]	99.4	9.9	1.2	52.9	9.5	2.2	n.d	n.d	23.7
8.0[b]	99.6	0.5	0.6	61.5	9.5	5.9	n.d	n.d	21.5

[a] C_6 = sum of sorbitol and mannitol, C_5 = xylitol, C_4 = erythritol, C_3 = 1,2propanediol, glycerol, C_2 = ethyleneglycol
[b] after a suplemetal mix-milling of 30 min

and the oligosaccharides produced) and the solid catalyst facilitated by the close proximity between different reacting species (i.e., catalyst, cellulose and the hydrogen species dissociated onto the metal surface) allows for the rapid hydrogenation of sugars. Accordingly, Fig. 10b shows how an additional 30 min amorphous cellulose-catalyst mix-milling pre-treatment enhanced the sorbitol yield from 37.6% to 52.9% at 4.0 MPa H_2. Furthermore, if the process was conducted at 8.0 MPa of H_2 pressure, the sorbitol production reached a yield as high as 61.5% (77.0% of total sugar alcohols and 15.5% of by-products). Considering this strategy, the best-suited catalytic results were achieved from mix-milled amorphous cellulose after 26 h at 190 ºC and 8.0 MPa H_2. Under such conditions, a sorbitol yield as high as 62% was achieved, with a 77% yield of total sugar alcohols. This productivity compares with the best data reported in the literature so far.

4. Conclusions

This work provides novel insights into the influence of a broad set of variables on the hydrothermal hydrogenation of cellulose using a Ni/CNF (10.7 wt% of Ni, mean diameter of 11.3 nm) catalyst. These included a first analysis addressing the impact of the duration of a ball-milling pre-treatment step and the influences of the hydrothermal time and temperature, and a second study covering the influence of mass transfer limitations. Increasing the ball-milling step drove the micro-crystalline cellulose to its amorphous state, with the final crystal index of this substrate influencing the effects of the temperature and time on the posterior hydrothermal hydrogenation process. The pre-treatment of cellulose not only promoted the dissolution and hydrolysis step but also enhanced the contact with metal catalysts for its rapid hydrogenation. This point became essential for preventing the cleavage reaction of (C-C and C-O) bonds from sugar intermediates. Additionally, the different influences of the temperature and processing time highlighted the importance of process control to promote the first transformation of cellulose into glucose and its subsequent hydrogenation to sorbitol to minimise the extension of side reactions. Despite finding appropriate conditions (a good combination of cellulose crystallinity and hydrothermal time and temperature), high sorbitol productions were still hindered by mass transfer limitations. On the bright side, these could be countered by including an additional mix-milling of the amorphous cellulose produced in the first pre-treatment with the catalyst and increasing the H_2 pressure of the hydrothermal hydrogenation process. This allowed attaining a sorbitol yield as high as 62% at 190 ºC using an

initial H_2 pressure of 8 MPa for 26 h, which is one of the best results reported in the literature. The detailed mechanistic understanding of the process presented in this work, along with the promising results achieved, not only provide a unified picture of the chemistry involved in the hydrolytic hydrogenation of cellulose using Ni-based catalysts but also can pave the way for the development of future biorefineries based on cellulose utilisation.

CRediT authorship contribution statement

I. Suelves: Conceptualization, Methodology, Project administration, Funding acquisition, Supervision, Writing – review & editing. **J.L. Pinilla:** Conceptualization, Methodology, Supervision, Project administration, Funding acquisition. **J. Remón:** Conceptualization, Methodology, Writing – review & editing, Validation, Investigation. E. Frecha: Validation, Investigation, Writing – original draft. **D. Torres:** Validation, Investigation, Writing – review & editing. **J.L. Pinilla:** Project administration, Funding acquisition. Writing – review & editing. All authors contributed to manuscript revision, read, and approved the submitted version.

Declaration of Competing Interest

The authors declare that they have no known competing financial interests or personal relationships that could have appeared to influence the work reported in this paper.

Data Availability

Data will be made available on request.

Acknowledgements

The authors are grateful for the financial support from the Spanish Ministry of Economy and Competitiveness (MINECO, Project ENE2017-83854-R) and the I+D+i project PID2020-115053RB-I00, funded by MCIN/ AEI/10.13039/501100011033. J.R. and D.T. are grateful to the Spanish Ministry of Science, Innovation and Universities for the Juan de la Cierva Incorporación (JdC-I) fellowships (Grant Numbers: IJC2018-037110-I and IJC2020-045553-I, respectively) awarded.

References

[1] J.N. Chheda, G.W. Huber, J.A. Dumesic, Liquid-phase catalytic processing of biomass-derived oxygenated hydrocarbons to fuels and chemicals, Angew. Chem. Int. Ed. 46 (38) (2007) 7164–7183.
[2] L. Petrus, M.A. Noordermeer, Biomass to biofuels, a chemical perspective, Green. Chem. 8 (10) (2006) 861–867.
[3] R.A. Sheldon, Green and sustainable manufacture of chemicals from biomass: state of the art, Green. Chem. 16 (3) (2014) 950–963.
[4] Z. Yuan, W. Dai, S. Zhang, F. Wang, J. Jian, J. Zeng, H. Zhou, Heterogeneous strategies for selective conversion of lignocellulosic polysaccharides, Cellulose 29 (6) (2022) 3059–3077.
[5] C. Chatterjee, F. Pong, A. Sen, Chemical conversion pathways for carbohydrates, Green. Chem. 17 (2014).
[6] Z. Sun, B. Fridrich, A. de Santi, S. Elangovan, K. Barta, Bright side of lignin depolymerization: toward new platform chemicals, Chem. Rev. 118 (2) (2018) 614–678.
[7] K. Kohli, R. Prajapati, B.K. Sharma, Bio-based chemicals from renewable biomass for integrated biorefineries, Energies 12 (2) (2019) 233.
[8] T. Werpy, J. Holladay, J. White, Top Value Added Chemicals From Biomass: I. Results of Screening for Potential Candidates from Sugars and Synthesis Gas, (2004).
[9] H. Kobayashi, A. Fukuoka, Synthesis and utilisation of sugar compounds derived from lignocellulosic biomass, Green. Chem. 15 (7) (2013) 1740–1763.
[10] A.M. Ruppert, K. Weinberg, R. Palkovits, Hydrogenolysis goes bio: from carbohydrates and sugar alcohols to platform chemicals, Angew. Chem. (Int. Ed. Engl.) 51 (11) (2012) 2564–2601.
[11] J. Zhang, J.-b Li, S.-B. Wu, Y. Liu, Advances in the catalytic production and utilization of sorbitol, Ind. Eng. Chem. Res. 52 (34) (2013) 11799–11815.
[12] S. Kumar, H. Ali, S.K. Kansal, A. Pandey, S. Saravanamurugan, Chapter 9 - sustainable production of sorbitol—a potential hexitol, in: S. Saravanamurugan, A. Pandey, H. Li, A. Riisager (Eds.), Biomass, Biofuels, Biochemicals, Elsevier, 2020, pp. 259–281.
[13] N. Akiya, P.E. Savage, Roles of water for chemical reactions in high-temperature water, Chem. Rev. 102 (8) (2002) 2725–2750.
[14] M. Yabushita, H. Kobayashi, A. Fukuoka, Catalytic transformation of cellulose into platform chemicals, Appl. Catal. B: Environ. 145 (2014) 1–9.
[15] A. Fukuoka, P.L. Dhepe, Catalytic conversion of cellulose into sugar alcohols, Angew. Chem. Int. Ed. 45 (31) (2006) 5161–5163.
[16] C. Luo, S. Wang, H. Liu, Cellulose conversion into polyols catalyzed by reversibly formed acids and supported ruthenium clusters in hot water, Angew. Chem. Int. Ed. 46 (40) (2007) 7636–7639.
[17] W. Deng, X. Tan, W. Fang, Q. Zhang, Y. Wang, Conversion of cellulose into sorbitol over carbon nanotube-supported ruthenium catalyst, Catal. Lett. 133 (1) (2009) 167.
[18] J. Pang, A. Wang, M. Zheng, Y. Zhang, Y. Huang, X. Chen, T. Zhang, Catalytic conversion of cellulose to hexitols with mesoporous carbon supported Ni-based bimetallic catalysts, Green. Chem. 14 (3) (2012) 614–617.
[19] S. Van de Vyver, J. Geboers, M. Dusselier, H. Schepers, T. Vosch, L. Zhang, G. Van Tendeloo, P.A. Jacobs, B.F. Sels, Selective bifunctional catalytic conversion of cellulose over reshaped ni particles at the tip of carbon nanofibers, ChemSusChem 3 (6) (2010) 698–701.
[20] H. Kobayashi, Y. Ito, T. Komanoya, Y. Hosaka, P.L. Dhepe, K. Kasai, K. Hara, A. Fukuoka, Synthesis of sugar alcohols by hydrolytic hydrogenation of cellulose over supported metal catalysts, Green. Chem. 13 (2) (2011) 326–333.
[21] L. Ribeiro, J.J.M. Órfão, M. Pereira, Comparative study of different catalysts on the direct conversion of cellulose to sorbitol, Green. Process. Synth. 0 (2015).
[22] I.C. Gerber, P. Serp, A theory/experience description of support effects in carbon-supported catalysts, Chem. Rev. 120 (2) (2020) 1250–1349.
[23] L.S. Ribeiro, J.J. Delgado, J.J. de Melo Órfão, M.F.R. Pereira, Direct conversion of cellulose to sorbitol over ruthenium catalysts: Influence of the support, Catal. Today 279 (2017) 244–251.
[24] F. Jérôme, S. Valange, Rational design of nanostructured carbon materials: contribution to cellulose processing, Nanotechnol. Catal. (2017) 627–654.
[25] E. Redina, O. Tkachenko, T. Salmi, Recent Advances in C5 and C6 sugar alcohol synthesis by hydrogenation of monosaccharides and cellulose hydrolytic hydrogenation over non-noble metal catalysts, Molecules 27 (4) (2022) 1353.
[26] Y. Feng, S. Long, X. Tang, Y. Sun, R. Luque, X. Zeng, L. Lin, Earth-abundant 3d-transition-metal catalysts for lignocellulosic biomass conversion, Chem. Soc. Rev. 50 (10) (2021) 6042–6093.
[27] G. Liang, L. He, H. Cheng, W. Li, X. Li, C. Zhang, Y. Yu, F. Zhao, The hydrogenation/dehydrogenation activity of supported Ni catalysts and their effect on hexitols selectivity in hydrolytic hydrogenation of cellulose, J. Catal. 309 (2014) 468–476.
[28] R. Reshmy, T.A.P. Paulose, E. Philip, D. Thomas, A. Madhavan, R. Sirohi, P. Binod, M. Kumar Awasthi, A. Pandey, R. Sindhu, Updates on high value products from cellulosic biorefinery, Fuel 308 (2022), 122056.
[29] P. Kumar, D.M. Barrett, M.J. Delwiche, P. Stroeve, Methods for pretreatment of lignocellulosic biomass for efficient hydrolysis and biofuel production, Ind. Eng. Chem. Res. 48 (8) (2009) 3713–3729.
[30] Y. Liao, B.O. de Beeck, K. Thielemans, T. Ennaert, J. Snelders, M. Dusselier, C. M. Courtin, B.F. Sels, The role of pretreatment in the catalytic valorization of cellulose, Mol. Catal. 487 (2020), 110883.
[31] L.S. Ribeiro, J.J.M. Órfão, M.F.R. Pereira, Enhanced direct production of sorbitol by cellulose ball-milling, Green. Chem. 17 (5) (2015) 2973–2980.
[32] Y. Liao, Q. Liu, T. Wang, J. Long, Q. Zhang, L. Ma, Y. Liu, Y. Li, Promoting hydrolytic hydrogenation of cellulose to sugar alcohols by mixed ball milling of cellulose and solid acid catalyst, Energy Fuels 28 (9) (2014) 5778–5784.
[33] E. Frecha, J. Remón, D. Torres, I. Suelves, J.L. Pinilla, Design of highly active Ni catalysts supported on carbon nanofibers for the hydrolytic hydrogenation of cellobiose, Front. Chem. 10 (2022).
[34] J.L. Pinilla, S. de Llobet, R. Moliner, I. Suelves, Ni-Co bimetallic catalysts for the simultaneous production of carbon nanofibres and syngas through biogas decomposition, Appl. Catal. B Environ. 200 (2017) 255–264.
[35] L. Segal, C.M. Conrad, J.J. Creely, A.E. Martin, An empirical method for estimating the degree of crystallinity of native cellulose using the X-ray diffractometer, Text. Res J. 29 (10) (1959) 786–794.
[36] S. Coseri, Cellulose: to depolymerize… or not to? Biotechnol. Adv. 35 (2) (2017) 251–266.
[37] T. Ennaert, B. Op de Beeck, J. Vanneste, A.T. Smit, W.J.J. Huijgen, A. Vanhulsel, P. A. Jacobs, B.F. Sels, The importance of pretreatment and feedstock purity in the reductive splitting of (ligno)cellulose by metal supported USY zeolite, Green. Chem. 18 (7) (2016) 2095–2105.
[38] J. Verendel, T. Church, P. Andersson, Catalytic one-pot production of small organics rom polysaccharides, Synthesis 2011 (2011) 1649–1677.
[39] T. Gagić, A. Perva Uzunalic, Ž. Knez, M. Škerget, Hydrothermal degradation of cellulose at temperature from 200 °C to 300 °C, Ind. Eng. Chem. Res. 57 (2018).
[40] S. Hunter, P. Savage, Recent advances in acid- and base-catalyzed organic synthesis in high-temperature liquid water, Chem. Eng. Sci. 59 (2004) 4903–4909.
[41] S.S. Toor, L. Rosendahl, A. Rudolf, Hydrothermal liquefaction of biomass: a review of subcritical water technologies, Energy 36 (5) (2011) 2328–2342.
[42] A. Bayu, A. Abudula, G. Guan, Reaction pathways and selectivity in chemo-catalytic conversion of biomass-derived carbohydrates to high-value chemicals: a review, Fuel Process. Technol. 196 (2019).

[43] O.V. Manaenkov, O.V. Kislitsa, V.G. Matveeva, E.M. Sulman, M.G. Sulman, L. M. Bronstein, Cellulose conversion into hexitols and glycols in water: recent advances in catalyst development, Front. Chem. 7 (834) (2019).
[44] X. Liu, X. Wang, S. Yao, Y. Jiang, J. Guan, X. Mu, Recent advances in the production of polyols from lignocellulosic biomass and biomass-derived compounds, RSC Adv. 4 (90) (2014) 49501–49520.
[45] E. Crezee, B.W. Hoffer, R.J. Berger, M. Makkee, F. Kapteijn, J.A. Moulijn, Three-phase hydrogenation of d-glucose over a carbon supported ruthenium catalyst—mass transfer and kinetics, Appl. Catal. A Gen. 251 (1) (2003) 1–17.